Available online at www.sciencedirect.com
SCIENCE DIRECT
International Journal of Heat and Mass Transfer 49 (2006) 3371–3378
International Journal of HEAT and MASS TRANSFER
www.elsevier.com/locate/ijhmt

Three-dimensional modeling of utility boiler pulverized coal tangentially fired furnace

Srdjan Belosevic [a,*], Miroslav Sijercic [a], Simeon Oka [a], Dragan Tucakovic [b]

[a] Institute of Nuclear Sciences "Vinca", Laboratory for Thermal Engineering and Energy, P.O. Box 522, 11001 Belgrade, Serbia and Montenegro
[b] Faculty of Mechanical Engineering, University of Belgrade, Kraljice Marije 16, 11120 Belgrade 35, Serbia and Montenegro

Received 15 November 2005
Available online 9 June 2006

Abstract

This paper presents selected results of numerical simulations of processes in utility boiler pulverized coal tangentially fired dry-bottom furnace. The simulations have been performed by specially developed comprehensive mathematical model. The main features of the model are a three-dimensional geometry, k–ε gas turbulence model, Eulerian–Lagrangian approach, particles-to-turbulence interaction, diffusion model of particle dispersion, six-flux method for radiation modeling and pulverized coal combustion model based on the global particle kinetics and experimentally obtained kinetic parameters. Five operation regimes of 210 MW_e boiler furnace burning Serbian lignites, with different grinding fineness of coal and coal quality, have been simulated. The model successfully predicts the influence of the parameters on the furnace processes and operation characteristics (like the flue gas temperature and the furnace walls radiation fluxes). The predicted flame temperature and percentage combustibles in bottom ash are in good agreement with the measurements. The developed model can find different applications, both in research and practice.

Keywords: Three-dimensional model; Tangentially fired furnace; Pulverized coal

1. Introduction

Pulverized coal tangentially fired furnaces are used extensively in power generation worldwide due to a number of their advantages, like uniform heat flux to the furnace walls and NO_x emission lower than in other firing types. Further study of the furnaces is needed by both experiments and simulations. While full-scale measurements are restricted by considerably high expenses, numerical simulation provides a cost-effective and powerful engineering tool, complementing experimental investigations. Because of the peculiar aerodynamics of the tangentially fired furnaces, the flow inside the furnaces [1], as well as the combustion processes, were found to be complicated for modeling. Still, comprehensive combustion models of large-scale tangentially fired furnaces, based on numerical solution of three-dimensional differential conservation equations, have been the subject of many investigations [2–8]. The models are similar in many ways to each other and to the model presented in this paper. The majority use variations of the SIMPLE algorithm and the k–ε gas turbulence model, or some derivatives, like RNG k–ε model [5] or k–ε–k_p two-phase turbulence model [6]. Gas phase conservation equations are mostly time-averaged, but some suggest the Favre-averaged equations instead [3]. A two-phase flow is usually described by Eulerian–Lagrangian approach and PSI-Cell method for coupling of phases, with some exceptions using Eulerian–Eulerian approach [8], or two-fluid trajectory model [6]. Most of the combustion submodels given in [2–8] treat particle devolatilization, char oxidation and additional gas phase reactions separately. Thermal radiation in the furnace is modeled by means of various approaches, like discrete transfer method [2], discrete ordinates method [3,6,7],

* Corresponding author. Tel.: +381 11 2458222x343; fax: +381 11 2453670.
E-mail address: v1belose@vin.bg.ac.yu (S. Belosevic).

0017-9310/$ - see front matter © 2006 Elsevier Ltd. All rights reserved.
doi:10.1016/j.ijheatmasstransfer.2006.03.022

Nomenclature

A	parameter in Arrhenius relation ($m\ s^{-1}$)
A	particle cross-section area (m^2)
b, f, s	scattering direction coefficients (–)
C_p	specific heat ($J\ kg^{-1}\ K^{-1}$)
$\mathscr{D}$	molecular diffusivity ($m^2\ s^{-1}$)
d	diameter (m)
E	activation energy of coal ($J\ kmol^{-1}$)
F	total radiation heat flux ($W\ m^{-2}$)
g	gravitational acceleration ($m\ s^{-2}$)
I	radiation intensity ($W\ m^{-2}$)
K	coefficient of radiation (m^{-1})
k	turbulence kinetic energy ($m^2\ s^{-2}$); reaction rate ($m\ s^{-1}$)
M	molar mass ($kg\ mol^{-1}$)
m	mass (kg)
N_p	particle concentration (particle number density (m^{-3}))
R	universal gas constant ($J\ kmol^{-1}\ K^{-1}$)
$\Re_p$	heterogeneous reaction rate ($kg\ s^{-1}$)
Sh	Sherwood number (–)
S_Φ	source term for general variable Φ
T	absolute temperature (K)
t	temperature (°C)
U_j	time-averaged velocity component ($m\ s^{-1}$)
$\vec{U}_p$	particle velocity vector ($m\ s^{-1}$)
U_{pdi}	particle diffusion velocity component ($m\ s^{-1}$)
XCO_2	mass concentration of carbon-dioxide ($kg\ kg^{-1}$)
x_j	coordinate in general index-notation (m)
x, y, z	Cartesian coordinates (m)

Greek symbols

Γ	diffusion coefficient ($m^2\ s^{-1}$)
Γ_{rd}	radiation diffusion coefficient (m)
ε	turbulence kinetic energy dissipation rate ($m^2\ s^{-3}$)
ν_p^t	particles turbulent diffusivity ($m^2\ s^{-1}$)
ν_t	fluid turbulent diffusivity ($m^2\ s^{-1}$)
ρ	density ($kg\ m^{-3}$)
σ_p	Prandtl–Schmidt number for particles (–)
τ	time (s)
τ_p	particle response time (s)
τ_t	gas phase Lagrangian integral time scale (s)
Φ	general variable
χ_p	mass concentration of gaseous products of combustion ($kg\ kg^{-1}$)
χ_{mol}^{ox}	oxidant molar concentration ($kmol\ m^{-3}$)
Ω_0	albedo of radiation scattering (–)

Subscripts

a	absorption
b	black body
d	diffusion
in	initial
p	particle
Res	resultant
r	radiation; kinetic reaction
s	scattering
t	turbulent; total
x, y, z	related to Cartesian coordinates

Superscript

t	turbulent

six-fluxes method [4], Monte Carlo method [5] and P-1 model [8]. Although commercial codes are applied successfully [7,8], research efforts are still given worldwide to specially developed comprehensive models of the furnaces [1–6].

This paper presents selected results of numerical simulations of processes in utility boiler pulverized coal tangentially fired dry-bottom furnace. The simulations of the processes are based on a comprehensive 3D differential mathematical model, specially developed for the purpose. The model offers such a composition of submodels and modeling approaches so as to balance submodel sophistication with computational practicality. A 3D geometry, Eulerian–Lagrangian approach, k–ε gas turbulence model, particles-to-turbulence interaction, diffusion model of particle dispersion, six-flux method for radiation modeling and pulverized coal particle combustion model based on the global particle kinetics and experimentally obtained coal kinetic parameters are the main features of the model. The furnace geometry is described in more detail in this paper than in some references [4,6], with burners simulated in great details, like in [1,7]. Diffusion model of particle dispersion by turbulence is applied, giving better computational efficiency than the stochastic models [2,5,7]. In contrast to [2–8], the effect of particles on gas turbulence is modeled as well. Due to the lack of experimental data for the case-study coals to consider more complex combustion mechanisms, a global model of particles combustion was selected, where all individual processes in a complex combustion process are treated together. Five operation regimes of 210 MW_e boiler furnace burning pulverized Serbian lignites, with different grinding fineness of coal and coal quality, have been predicted. The influences of the parameters on the furnace processes have been investigated and selected predictions compared with the full-scale measurements. Parametric calculations and the comparisons

present a validation of the comprehensive model and demonstrate its applicability.

2. The case-study furnace geometry and operating conditions

The case-study boiler unit is A2 unit of Nikola Tesla power plant (Serbia), with natural water-steam circulation and tangentially fired dry-bottom furnace. The unit generates a nominal steam capacity of 650 t/h and electrical output of 210 MW_e. The case-study furnace has six jet burners, each connected to one coal mill. The geometrical model of the furnace is shown in Fig. 1. Pulverized coal–air mixture at 165 °C from the coal mill enters the furnace through 8 rectangular ducts, while the secondary air at 270 °C is injected through the ducts above, between and beneath. Cross-sections at entrance of the coal–air duct and for the entire burner are (0.51×1.23) m and (6.5×1.23) m.

The operation of the case-study furnace was considered in stationary conditions. Five operation regimes with different grinding fineness of coal and coal quality were predicted. For coal Kolubara-Field "D" the grinding finenesses of $R_{90} = 48.4\%$, 60.15% and 73.85% were considered and, in addition, the grinding fineness of $R_{90} =$ 73.85%, for coals Kolubara-Tamnava and Kostolac-Drmno. R_{90} denotes percentage residue on sieve with grid spacing of 90 μm. The nominal-load operating conditions (five burners operating) of the furnace are given in Table 1. Existing distribution of coal particle sizes is represented by using five different size classes of pulverized coal, given in Table 2. Coal particle density is 1300 kg/m^3. For the case-study coals, proximate and ultimate analyses, as well as the heating value and kinetic parameters, are given in Table 3. The compositions of pulverized coals have been calculated for the moisture content of 14%.

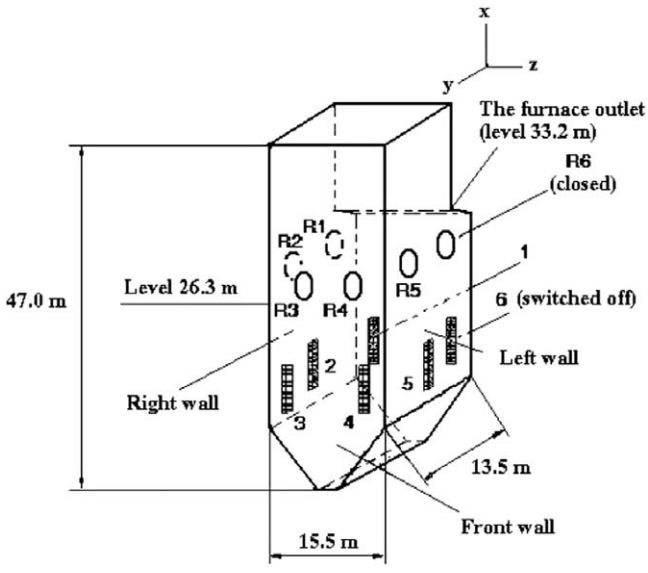

Fig. 1. Geometrical model of A2 210 MW_e boiler unit furnace: 1, 2, 3, 4, 5, 6 – burners, R1, R2, R3, R4, R5, R6 – recirculation holes.

Table 1
Nominal-load operating conditions of the case-study furnace

Coal mills operating	1, 2, 3, 4, 5
Total coal feed rate (t h^{-1})	265
Pulverized coal mass flow rate per burner (t h^{-1})	53
Total air flow rate (m^3 h^{-1})	660 000
Excess air, measured at the furnace outlet (–)	1.3–1.4
Temperature of pulverized coal–air mixture transport fluid (°C)	165
Total mass flow rate of coal–air mixture transport fluid, per burner (kg s^{-1})	30.51
Total volume flow rate of the mixture transport fluid, per burner (m^3 h^{-1})	135 600
Primary air (m^3 h^{-1})	37 000
Recirculating gases (m^3 h^{-1})	66 000
Evaporated moisture (m^3 h^{-1})	32 600
Secondary air temperature (°C)	270
Secondary air mass flow rate, per burner (kg s^{-1})	17.01
Secondary air volume flow rate, per burner (m^3 h^{-1})	95 000
Recirculating gases temperature (°C)	900
Recirculating gases mass flow rate, per burner (kg s^{-1})	5.46

Table 2
The percentage of various size classes of pulverized coal for different grinding fineness

	Particle diameter (μm)				
	25	70	145	350	850
Percentage for $R_{90} = 48.4\%$	40.68	10.92	20.74	17.84	9.82
Percentage for $R_{90} = 60.15\%$	24.83	13.95	28.90	21.47	10.85
Percentage for $R_{90} = 73.85\%$	7.55	18.60	31.43	25.10	17.32

Table 3
Composition, heating value and kinetic parameters for the case-study coals

	Coal		
	Kolubara-Field "D"	Kolubara-Tamnava	Kostolac-Drmno
Proximate analysis (as received)			
Moisture (%)	52.67	51.10	38.60
Ash (%)	11.23	15.87	28.39
Volatile (%)	21.46	19.07	23.36
Fixed carbon (%)	14.64	13.96	9.65
Lower heating value (as received)			
Heating value (kJ kg^{-1})	7816	7372	7017
Ultimate analysis (as received)			
Carbon (%)	22.70	20.59	20.54
Hydrogen (%)	2.13	1.87	1.97
Oxygen (%)	10.39	9.77	9.36
Nitrogen (%)	0.50	0.40	0.50
Sulfur (%)	0.39	0.40	0.64
Kinetic parameters and Arrhenius reaction rates at 1273 K			
A (m s^{-1})	8.9×10^3	9.03×10^3	5.5×10^3
E (kJ kmol^{-1})	9.54×10^4	9.71×10^4	9.95×10^4
Reaction rate (m s^{-1})	1.08	0.93	0.45

3. Mathematical model and numerical method

The developed comprehensive model [9–11] extended available submodels by describing fully the 3D flow, combustion and heat transfer in existing geometry, with indetails modeling of the interactions between turbulence and particles and by including chemical kinetics of the coals considered and real coal particle size distribution.

Turbulent flow of multicomponent gaseous phase is described by time-averaged Eulerian partial differential conservation equations for mass, momentum, energy, concentrations of gaseous components, as well as the turbulence kinetic energy and its rate of dissipation. For general variable Φ

$$\frac{\partial}{\partial x_j}(\rho U_j \Phi) = \frac{\partial}{\partial x_j}\left(\Gamma_\Phi \frac{\partial \Phi}{\partial x_j}\right) + S_\Phi + S_\mathrm{p}^\Phi \tag{1}$$

Standard k–ε gas turbulence model is extended to a 3D case. For coupling of phases PSI Cell method is used, with additional sources due to particles S_p^Φ. The effect of particles-to-gas turbulence is modeled by additional sources for k and ε.

Dispersed phase is described by differential equations of motion, energy and mass change in Lagrangian field, with diffusion model of particle dispersion by turbulence. Particle velocity is a sum of convective and diffusion velocity:

$$\vec{U}_\mathrm{p} = \vec{U}_\mathrm{pc} + \vec{U}_\mathrm{pd} \tag{2}$$

The convective velocity is obtained from the equation of motion, by particle tracking along the trajectories with constant particle number density. The dispersion is modeled by introducing the particle diffusion velocity. Inter-particle collisions are neglected and wall-to-particle collisions are supposed to be elastic. Diffusion velocity is given as

$$\vec{U}_\mathrm{pd} = -\frac{1}{N_\mathrm{p}}\Gamma_\mathrm{p}\nabla N_\mathrm{p}, \quad U_{\mathrm{pd}_i} = -\frac{1}{N_\mathrm{p}}\Gamma_\mathrm{p}\frac{\partial N_\mathrm{p}}{\partial x_i} \tag{3}$$

Particle concentration N_p (particle number density) is obtained from the equation in the form of Eq. (1). Coefficient of particle turbulent diffusion Γ_p is given with respect to the fluid and particles turbulent diffusivity, ν_t and $\nu_\mathrm{p}^\mathrm{t}$, with $\sigma_\mathrm{p} = 1.3$–1.6:

$$\Gamma_\mathrm{p} = \frac{\nu_\mathrm{p}^\mathrm{t}}{\sigma_\mathrm{p}}, \quad \nu_\mathrm{p}^\mathrm{t} = \nu_\mathrm{t}\cdot\left(1+\frac{\tau_\mathrm{p}}{\tau_\mathrm{t}}\right)^{-1} \tag{4}$$

The six-flux method is used to model thermal radiation [12]. The model considers a three-dimensionality of radiation and anisotropy of radiation scattering. Equations for the total radiation flux components F_x, F_y and F_z are solved simultaneously with the fluid dynamic equations by the same numerical procedure. In x-direction,

$$\frac{1}{K_\mathrm{t}}\frac{\mathrm{d}}{\mathrm{d}x}\left(\Gamma_\mathrm{rd}\frac{\mathrm{d}F_x}{\mathrm{d}x}\right) = -(1-\Omega_0\mathrm{f}-\Omega_0\mathrm{b})F_x + 2\Omega_0\mathrm{s}(F_y+F_z) + (1-\Omega_0)\frac{I_\mathrm{b}}{3} \tag{5}$$

Eq. (5) has an equivalent form for y- and z-directions. Source terms due to radiation are added in the gas phase and dispersed phase energy equations.

Individual processes in complex combustion process are treated together on the basis of global particle kinetics and experimentally obtained coal kinetic parameters. The methodology is general and could be adapted without difficulties to include additional reactions. The model considers heterogeneous reactions on the basis of the char combustion model and within a "shrinking core" concept [13]. Coal particle mass change, equal to the reaction rate, is given in combined kinetic-diffusion regime:

$$-\frac{\mathrm{d}m_\mathrm{p}}{\mathrm{d}\tau} = \Re_\mathrm{p} = \frac{A_\mathrm{p}M_\mathrm{p}\chi_\mathrm{mol}^\mathrm{ox}}{\frac{1}{k_\mathrm{r}}+\frac{1}{k_\mathrm{d}}} \tag{6}$$

$$k_\mathrm{r} = \mathrm{A}\mathrm{e}^{-\frac{\mathrm{E}}{\mathrm{R}T}}, \quad k_\mathrm{d} = Sh\cdot\mathscr{D}/d_\mathrm{p}, \quad \mathscr{D} = 9.8\cdot10^{-10}\cdot T^{1.75} \tag{7}$$

where k_r is Arrhenius reaction rate in kinetic regime and k_d is diffusion parameter of mass transfer. Molecular diffusivity $\mathscr{D}$ is given by empirical expression for high-temperature combustion products [14]. Total particle mass change due to reactions is the sum of changes due to the individual processes. The reactions of complete oxidation of carbon and hydrogen are considered by the corresponding reaction rates, while sulfur is taken into account through equivalent carbon content. The rates of moisture evaporation and a consumption of oxygen from coal are taken as being proportional to the carbon oxidation rate. Mass and heat addition due to combustion is considered by additional sources in the conservation Eq. (1).

Initial and boundary conditions usual in modeling practice for elliptical partial differential equations are applied. Boundary conditions at the inlet are defined by the nature of the problem and at the outlet by the condition of continuity. Conditions near the walls are described by the "wall functions". The wall heat flux is assumed to change along the furnace and the boundary condition of constant wall temperature is used.

The gas phase properties are determined with respect to the equations of state, semiempirical relations and regressions. Specific heat of the particle is given by an empirical expression:

$$C_{pp} = 832.2 + 0.489(T-130) \tag{8}$$

SIMPLE calculation algorithm is used for coupling of the continuity and the momentum equations. The control volume method and hybrid-differencing scheme [15] are used for casting the differential equations into a system of linear algebraic equations. For solving the system, a modification of SIP method is used. Stabilization of iteration procedure is achieved by under-relaxation. The staggered numerical grid with $75\times34\times41 = 104550$ grid nodes has been applied and adapted to the flow character. From each of the 5 burners, 80 particle trajectories have been numerically tracked for each of the 5 size classes, giving the total number of 2000 particle trajectories considered.

4. Results and discussion

Essential characteristics of the tangentially fired furnace aerodynamics is the central vortex. As shown in the predictions (Fig. 2), the vortex is moved toward the switched off burner, effecting the flame position and temperature field in the furnace and the heat fluxes distribution at the furnace walls.

A demonstration of the model application in optimizing the scheme of switching off the burners is given in Fig. 3, for a simplified case, in which the combustion is completed at the inlet, producing hot gases entering the furnace. Considering temperature field symmetry (good for combustion and reduction of surface fouling), it is better to switch off the opposite burners than the neighboring ones.

4.1. Parametric calculations

Five operation regimes of the case-study furnace, with different grinding fineness of coal and coal quality, have been predicted and the influences of the parameters to the furnace processes investigated.

Pulverized coal particles diameter change due to combustion for 2 particle size classes of 2 coals and grinding fineness of $R_{90} = 73.85\%$, is shown in Fig. 4. The level to which the combustion of particles continues effects the flame vertical position and thermal loading of the furnace screen walls. Particles change their diameter while the combustion takes place. Combustion of smaller particles is completed more rapidly and the particles move to the furnace exit as flying ash. As expected, combustion of larger particles lasts longer. Coal with finer grinding has more small particles so the conversion of small size classes due to combustion will dominate. Combustion of both size classes of coal Kostolac-Drmno terminates at higher levels,

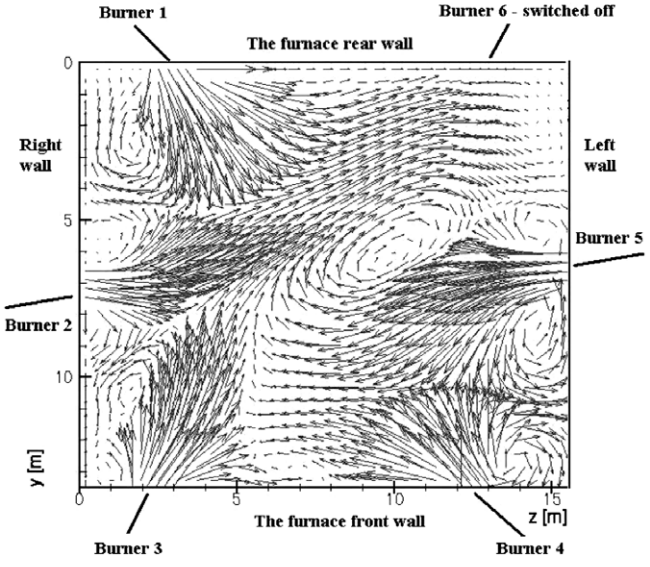

Fig. 2. Predicted central vortex in the furnace.

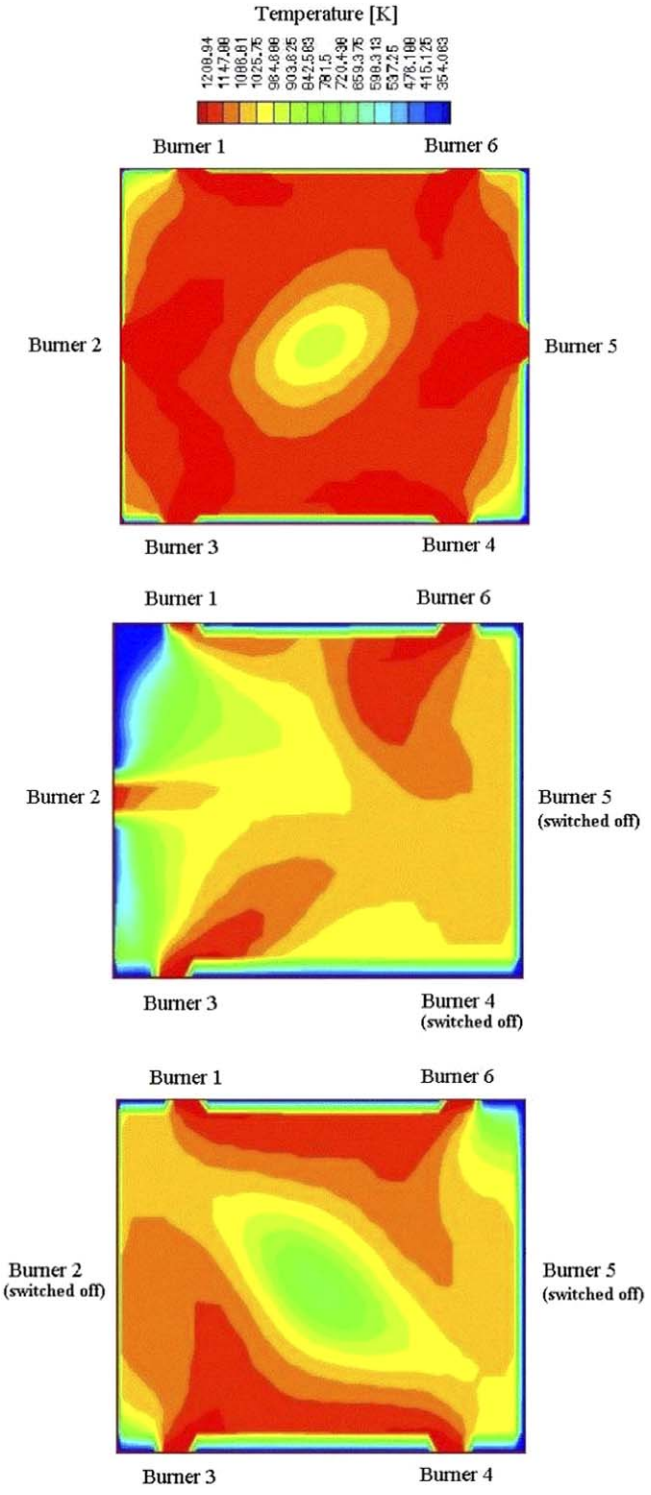

Fig. 3. Influence of the burners switching off to the furnace temperature field.

because of considerably smaller values of reaction rate, compared to Kolubara-Field "D" (Table 3). Higher ash content (Table 3) gives larger diameter of ash particles remaining after the complete combustion in the case of Kostolac-Drmno coal.

Influence of grinding fineness of coal to the furnace processes is illustrated in Fig. 5 as the change of cross-section

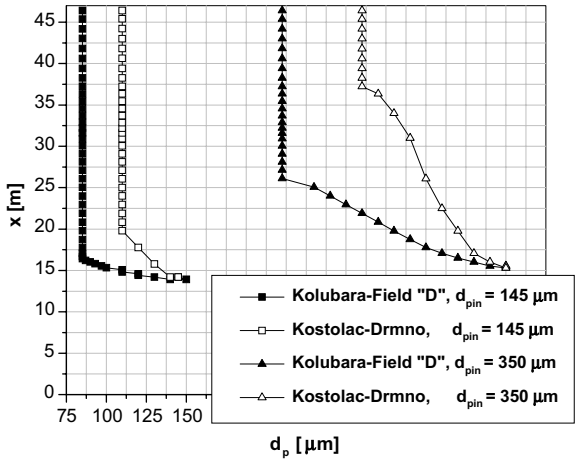

Fig. 4. Coal particle diameter change due to combustion in the furnace for 2 coals and 2 particle size classes.

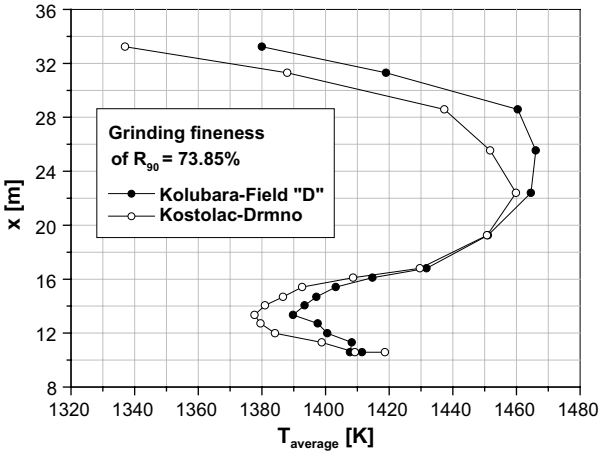

Fig. 6. Change of the flue gas temperature for different coals.

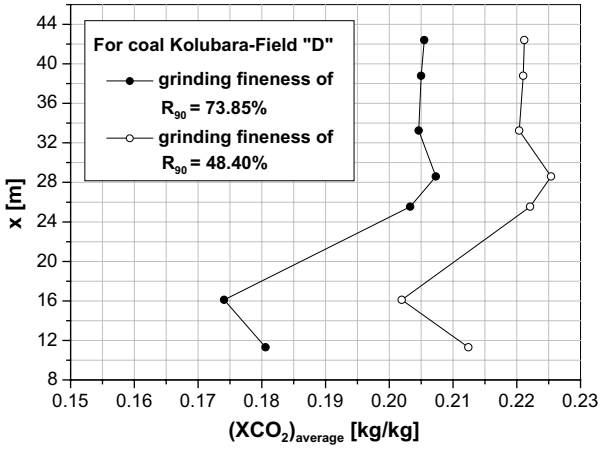

Fig. 5. Change of CO_2 mass concentration for different grinding fineness of coal.

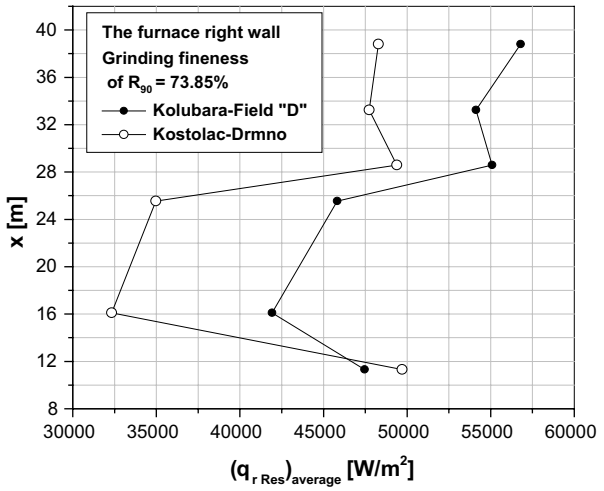

Fig. 7. Change of the radiation flux at the right furnace wall for different coals.

averaged CO_2 mass concentration along the furnace. For finer grinding, there are more particles of small size classes that will burn rapidly, giving higher concentrations at all levels. Also, there are not so many large particles going to the hopper, but a number of particles moving upwards and giving higher CO_2 concentration in the central region. Combustion products content grows to the level near the one at which the combustion is finished.

Changes of cross-section averaged flue gases temperature and radiation heat flux at the furnace right wall are given in Figs. 6 and 7, in dependence on the coal quality. Fig. 7 presents the resultants of predicted radiation flux components, cross-section averaged for each level. Since combustion of coal Drmno is finished at higher level than for coal Kolubara-Field "D" (Fig. 4), Drmno will give lower values of both the temperature and the radiation flux. This is also due to a considerably lower content of combustibles in coal Drmno (Table 3). Above the burners (17.0 m), temperature increases due to reactions until they are finished and then decreases because of radiation heat transfer increase. Due to lower content of combustible and a slower combustion, Kostolac-Drmno coal gives lower values of the fluxes.

4.2. Comparisons of the predictions with the full-scale measurements

Selected predictions for the furnace burning Kolubara-Field "D" coal, with the grinding fineness of $R_{90} = 73.85\%$, are compared with the full-scale measurements [16].

Fig. 8 presents predicted and measured values of the flame temperatures, at the level 26.3 m, along the furnace left wall (Fig. 1). The temperatures were measured by optical pyrometer, that did not measure the local temperature but the observed maximum temperature, depending on the flame transparency. Measured temperature is higher than the flame temperature near the wall and, to some extent, lower than the maximum temperature in the flame at the level. Predicted gas temperatures do not change

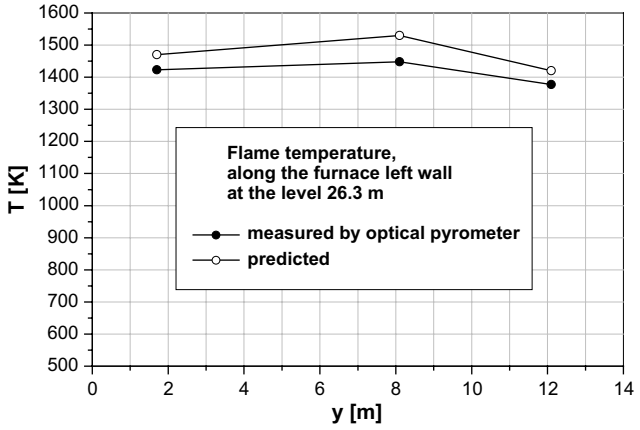

Fig. 8. The flame temperature change along the furnace left wall at the level 26.3 m.

considerably for distances larger than 0.25 m from the wall [11], so in Fig. 8 gas temperatures are presented at this distance. The model gives asymmetrical temperature distribution as the measurements, with maximum around the middle of the wall, due to the central vortex (and the flame) displacement towards the switched off burner (Fig. 2). Maximum measured temperatures relate to the level of 26.3 m [16], in the region of intensive heat release and the model predicts temperature maximum at 25.5–26.0 m.

Important characteristic of the furnace operation is loss due to unburnts in the bottom ash, that can be estimated by the developed model and the corresponding calculations [11]. The bottom ash is considered to be formed by the particles that fall beneath the horizontal plane at the half of the hopper height. The predictions for percentage combustibles in bottom ash and the bottom ash residue on sieve R_{90} (Table 4), are in good agreement with the measurements [17]. Predictions also show that a number of the largest particles (74%) fall into the hopper and the percentage of incompletely burnt particles is 65.43%. The amount of large particles within the bottom ash is considerably greater than in the initial coal particle size distribution (Table 2), meaning that "coarse" grinding fineness of coal is the main cause of losses due to the unburnts in bottom ash, which is in accordance with the exploitation experience.

Table 4
Percentage combustibles in bottom ash

	Coal or coal blend		
	Field "D", or 30% Field "D"/70% Tamnava[a]	30% Field D"/70% Tamnava[b]	Field "D"[c]
Boiler output (MW_e)	–	200	210
Coal consumption (t h^{-1})	–	240/281	265
Moisture (%)	–	50.72	52.67
Ash (%)	–	10.86	11.23
Lower heating value (as received) (kJ kg^{-1})	7335–7729	8344	7816
R_{90}, pulverized coal (%)	–	67.2	73.85
R_{90}, bottom ash (%)	–	97.0	91.605
Percentage combustibles in bottom ash (%)	54.4–68.8	66	57.06

[a] Operational investigations [17].
[b] Investigations on A2 unit after overhaul [17].
[c] Predicted by the developed model for the case-study furnace.

4.3. The convergence and the numerical grid effect

A 3D numerical grid with 104,550 grid nodes has been applied to provide the convergence and accuracy of the solutions and, in the same time, to meet the restrictions in computational time. Special grid refinements and computational procedures are employed to handle the near burners region and the furnace hopper. The grid has given a satisfactorily good convergence, especially with respect to the problem complexity. For a simplified case of monophase turbulent flow with heat transfer, the analysis of the numerical grid effect has shown that all applied grids give a good convergence: with 37,100 nodes in the half of the furnace, with 70,490 nodes in the whole furnace and 80,256 nodes for the furnace and crossover pass. The calculations have emphasized the importance of numerical particle tracking for general solution convergence.

5. Conclusions

Selected results of numerical simulations of processes in the utility boiler pulverized coal tangentially fired dry-bottom furnace, are presented in the paper. The simulations are based on a specially developed comprehensive 3D mathematical model. The model extended available submodels by describing the fully three-dimensional flow, combustion and heat transfer in existing geometry, with in-details modeling of particles-to-turbulence interactions and by including chemical kinetics of the coals considered. Five operation regimes of the case-study furnace, with different grinding fineness of coal and coal quality, have been simulated. The model successfully predicts the influence of the parameters to the furnace processes. The selected predictions are compared with the full-scale measurements, giving a satisfactorily good agreement. The grid applied provides a good convergence of the solutions. The parametric calculations and the comparisons present a validation of the model and demonstrate its applicability. The applications of the model can be expected in research, as a complement of experiments, full-scale measurements and engineering calculations, in prediction of the furnace operating situations and in power plant exploitation and control.

Acknowledgement

This work has been supported by the Ministry of Science and Environmental Protection (Republic of Serbia), within the Ministry projects.

References

[1] B. He, M. Chen, Q. Yu, S. Liu, L. Fan, S. Sun, J. Xu, W.P. Pan, Numerical study of the optimum counter-flow mode of air jets in a large utility furnace, Comput. Fluids 33 (9) (2004) 1201–1223.

[2] R.K. Boyd, J.H. Kent, Three-dimensional furnace computer modelling, in: Proceedings of the Twenty-first Symposium (International) on Combustion, The Combustion Institute, 1986, pp. 265–274.

[3] C.H. Scott, L.D. Smoot, A comprehensive three-dimensional model for simulation of combustion systems: PCGC-3, Energy Fuels 7 (6) (1993) 874–883.

[4] A. Bermudez de Castro, J.L. Ferin, Modelling and numerical solution of a pulverized coal furnace, in: Proceedings of the 4th International Conference on Technologies and Combustion for Clean Environment, Lisbon, Portugal, 1997, paper 33.1, pp. 1–9.

[5] J. Fan, L. Qian, Y. Ma, P. Sun, K. Cen, Computational modeling of pulverized coal combustion processes in tangentially fired furnaces, Chem. Eng. J. 81 (1–3) (2001) 261–269.

[6] L.X. Zhou, L. Li, R.X. Li, J. Zhang, Simulation of 3-D gas-particle flows and coal combustion in a tangentially fired furnace using a two-fluid-trajectory model, Powder Technol. 125 (2–3) (2002) 226–233.

[7] C. Yin, S. Caillat, J.L. Harion, B. Baudoin, E. Perez, Investigation of the flow, combustion, heat-transfer and emissions from a 609 MW utility tangentially fired pulverized coal boiler, Fuel 81 (8) (2002) 997–1006.

[8] R.V. Filkoski, I.J. Petrovski, A.T. Nospal, CFD simulation of processes in pulverized coal-fired boiler furnace, in: Proceedings on CD-ROM of full texts of the 15th International Congress of Chemical and Process Engineering CHISA 2002, ISBN: 80-86059-33-2, Praha, Czech Republic, 2002, pp. 1–10.

[9] S.V. Belosevic, S.N. Oka, M.A. Sijercic, Development of three-dimensional mathematical model for pulverized coal boiler furnaces, in: Book of Abstracts of the 3rd International FORTWIHR Conference 2001, Erlangen, Germany, 2001, pp. 1–4.

[10] S.V. Belosevic, S.N. Oka, M.A. Sijercic, Results of three-dimensional mathematical model development for pulverized coal furnace, in: Proceedings of the XIII Seminar of Young Scientists Physical Principles of Experimental and Mathematical Simulation of Heat and Mass Transfer and Gas Dynamics in Power Plants, vol. 1, MPEI Publishers, Saint Petersburg, Russia, 2001, pp. 254–257.

[11] S. Belosevic, Contribution to the modeling of processes in pulverized coal combustion boiler furnace, Ph.D. thesis, University of Belgrade, Belgrade, 2003 (in Serbian).

[12] C.H. Hottel, F.A. Sarofim, Radiative Transfer, McGraw-Hill, New York, 1967.

[13] L.D. Smoot, P.J. Smith, Coal Combustion and Gasification, Plenum Press, New York, 1985.

[14] T.V. Vilenskij, D.M. Hemaljan, Dynamics of Pulverized Fuel Combustion, Energija, Moscow, 1978 (in Russian).

[15] S.V. Patankar, Numerical Heat Transfer and Fluid Flow, Hemisphere, New York, 1980.

[16] P. Pavlovic, J. Riznic, Results of thermal measurements in the furnace of the power plant Nikola Tesla boiler No. 2, Report IBK-LTFT-104, Institute of Nuclear Sciences "Vinca", Belgrade-Vinca, Serbia and Montenegro, 1977 (in Serbian).

[17] P. Radulovic, Reduction of loss due to the unburnts in bottom ash, in boiler units of Nikola Tesla power plant, Report IBK-ITE-313, Institute of Nuclear Sciences "Vinca", Vinca, Serbia and Montenegro, November 1981 (in Serbian).